

## Time-resolved study of dephasing mechanisms of excitons in GaAs/Al<sub>x</sub>Ga<sub>1-x</sub>As quantum-well structures

Huib J. Bakker and Karl Leo

*Institut für Halbleitertechnik II, Rheinisch-Westfälische Technische Hochschule Aachen, D-52056 Aachen, Germany*

Jagdeep Shah

*AT&T Bell Laboratories, Holmdel, New Jersey 07733*

Klaus Köhler

*Fraunhofer-Institut für Angewandte Festkörperphysik, D-79108 Freiburg, Germany*

(Received 21 October 1993)

We present an experimental and theoretical study of the dephasing of heavy-hole excitons in a 70-Å GaAs/Al<sub>x</sub>Ga<sub>1-x</sub>As multiple-quantum-well structure. We measure the time-integrated three-pulse four-wave-mixing signal of heavy-hole excitons in the quantum-well sample. We model the third-order nonlinear optical response incorporating the effects of a stochastic modulation of the transition frequency. We find that the dephasing of the nonlinear polarization is mainly the result of a spectral-migration process of the excitons and, to a lesser extent, due to a homogeneous dephasing process. The time dependence of the four-wave-mixing signal is very well described by theory if the spectral-migration process is assumed to be energy dependent.

### I. INTRODUCTION

Time-resolved optical techniques are a powerful tool to study the dynamics of excitations in semiconductors.<sup>1,2</sup> One technique that is particularly sensitive to probe the dynamics of coherent excitations is time-integrated four-wave mixing (FWM). In this technique, a sequence of two or three pulses creates a third-order nonlinear optical polarization. The time-integrated measurement of the light generated by this polarization as a function of the delays between the pulses provides valuable information on the mechanisms that lead to a decay of the polarization and the population.

The dephasing of excitons in high-quality bulk GaAs and GaAs/Al<sub>x</sub>Ga<sub>1-x</sub>As quantum wells has been investigated previously with the two-pulse self-diffracted FWM technique.<sup>3-5</sup> In these studies, it was assumed that the relaxation is exponential with a homogeneous dephasing time constant  $T_2$ . Both in bulk GaAs and GaAs/Al<sub>x</sub>Ga<sub>1-x</sub>As quantum wells, the value of  $T_2$  was found to be a few picoseconds at low temperature (2 K) and low densities ( $< 1 \times 10^{15} \text{ cm}^{-3}$  in bulk and  $< 1 \times 10^9 \text{ cm}^{-2}$  in quantum wells). The value of  $T_2$  was found to decrease with increasing density and temperature. With the same self-diffracted FWM technique, the phase relaxation of free carriers in GaAs has been investigated.<sup>6</sup> The relaxation times of free carriers are found to be very short (20–50 fs) and are determined by carrier-carrier scattering.

The decay of the polarization is due to interactions of the excited system with its surroundings. These interactions will lead to a stochastic modulation of the transition frequency within a certain spectral distribution.<sup>7-9</sup>

In most experimental studies, it is assumed that the frequency fluctuation processes are either infinitely fast, leading to homogeneous broadening described with a phase relaxation time constant  $T_2$ , or infinitely slow, leading to inhomogeneous broadening. However, effects of a spectral fluctuation on a picosecond time scale have been observed both in time-resolved<sup>10</sup> and in frequency-resolved three-pulse FWM experiments,<sup>11</sup> showing that the frequency fluctuation is not always infinitely fast or slow. In addition to these observations, a strong non-exponential decay has been observed in time-integrated FWM experiments on dye molecules in solution,<sup>12,13</sup> also indicating that the rate of the fluctuations can be intermediate.

In this paper, we investigate in detail with time-integrated three-pulse FWM the mechanisms that induce the dephasing of heavy-hole excitons in a GaAs/Al<sub>x</sub>Ga<sub>1-x</sub>As multiple-quantum-well structure. We show that the dephasing of excitons cannot simply be described as a homogeneous or inhomogeneous dephasing process. We find that the relaxation is dominated by a frequency-fluctuation process that takes place on a picosecond time scale.

This paper is organized as follows. In Sec. II we describe the experimental setup. In Sec. III we present a model that describes the effects of a stochastic modulation of the transition frequency on the relaxation. In Sec. IV the experimental and calculated results are presented and discussed, and in Sec. V we present the conclusions.

### II. EXPERIMENT

We perform time-integrated three-pulse FWM experiments on a sample that contains ten 70-Å GaAs quantum

wells. The sample is grown without growth interruption at the interfaces, which prevents the formation of larger areas with constant well thickness. The quantum wells are part of a double-well structure, which contains a 70-Å and a 45-Å quantum well separated by a 50-Å barrier. The electronic states in the double well are out of resonance at zero applied voltage (as in the present experiment). The lowest electronic state of the 70-Å-wide well investigated here does not have a relaxation channel to the other well. The double-well systems are separated by thick (20-nm)  $\text{Al}_{0.35}\text{Ga}_{0.65}\text{As}$  barriers. The well thickness is determined by photoluminescence (PL) and photoluminescence-excitation (PLE) measurements and agrees very well with the design value. The sample was glued on a Sapphire disk and the substrate was removed by standard wet-etching techniques to allow transmission experiments. In the PL and PLE experiments, the sample showed a rather broad  $n=1$  heavy-hole exciton transition (full width at half maximum  $\approx 3\text{--}4$  meV).<sup>14</sup> The shift between PL and PLE (Stokes shift) is on the same order of magnitude.

The time-resolved experiments were performed with a tandem synchronously pumped dye-laser system described previously<sup>14</sup> that creates pulses of 400–500 fs pulse width, tunable between 700 and 815 nm. Figure 1 shows the schematical experimental setup. The pulse train is split into three parts that are focused to a single spot into the sample that is located on the cold finger of a He-flow cryostat. All three beams are copolarized. The temperature can be adjusted from about 10 K to room temperature. The intensity of the laser pulses is attenuated to reach the regime where the rate of decay of the four-wave-mixing signal becomes independent on the excitation power. This corresponds to an excitation density of about  $5 \times 10^8$  excitons  $\text{cm}^{-2}$ . In the three-pulse FWM experiment, the first pulse that enters the sample creates a linear polarization. The second pulse will transfer this polarization into a population grating from which the third pulse is diffracted in the direction  $k_4 = k_3 + k_2 - k_1$ . The time-integrated signal in this direction is measured as a function of the delay times

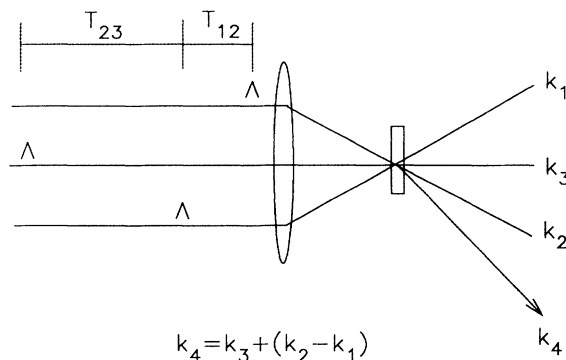


FIG. 1. Experimental configuration for a three-pulse four-wave-mixing experiment. Pulse 1 creates a linear polarization, pulse 2 transfers this polarization into a population grating with wave vector  $k_2 - k_1$ , from which the third pulse is diffracted in the direction  $k_3 + k_2 - k_1$ .

$T_{12}$  between pulses 1 and 2 and  $T_{23}$  between the pulses 2 and 3. The signal is measured by a standard lock-in technique and read out by a personal computer. The background signal due to scattering of the transmitted beams 1, 2, and 3 is determined by measuring the signal at large negative delays for which no diffracted signal will be present. This background signal is subtracted from the measured transients.

### III. MODEL FOR STOCHASTIC MODULATION IN THREE-PULSE FOUR-WAVE MIXING

#### A. Introduction

In this section we describe a model that accounts for the effects of a fluctuation of the transition frequency on the time evolution of the linear polarization, the population grating, and the third-order polarization that are formed in a three-pulse FWM experiment. The rate of the fluctuations of the transition frequency can be defined by the inverse of a correlation time constant  $T_c$ <sup>3</sup>:

$$\langle \delta\omega(t)\delta\omega(0) \rangle = D^2 e^{-t/T_c}, \quad (3.1)$$

where  $\delta\omega$  is the detuning of a single excitation from the maximum of the spectral distribution,  $D$  is the width of the spectral distribution, and the angular brackets indicate an ensemble average. The decay of the polarization is determined by both the correlation time constant  $T_c$  and the spectral width  $D$ . When the time constant  $T_c$  is very long compared to the inverse spectral width, the polarization will predominantly decay as a result of the dephasing of the different frequency components of the spectral distribution. In this case, the spectral line is inhomogeneously broadened and for a Gaussian shaped spectral distribution the linear polarization will show a Gaussian decay with a time constant  $\tau_{\text{inh}} = D^{-1}$ . In this inhomogeneous limit, the experimentally measured absorption band will be the same as the spectral distribution. If the phase of the oscillator is conserved when the transition frequency changes, the decay of the polarization will become slower with decreasing  $T_c$  and the measured absorption line will become narrower (motional narrowing). When  $T_c$  is much smaller than the inverse spectral width, the polarization at all frequency components within the spectral width will decay exponentially with a time constant  $T_2$  that is proportional to  $T_c^{-1}$ . In this limit, the absorption line is homogeneously broadened. When  $T_c$  is of the same order as the inverse spectral width, the broadening of the absorption line is in between homogeneous and inhomogeneous and the decay of the polarization can become strongly nonexponential.

The frequency-fluctuation processes that induce the dephasing are known in the literature as Kubo-Anderson processes.<sup>8,9</sup> In such a Kubo-Anderson process it is assumed that the transition frequency changes instantaneously after a characteristic time  $\delta\tau$  within a stationary distribution. This distribution is often taken to be Gaussian. The change of the transition frequency can

be the result of many successive small frequency jumps (weak modulation limit),<sup>8,15–26</sup> which means that the frequency after such a jump is strongly correlated to the frequency before the jump. However, the change of the transition frequency can also result from large jumps of the transition frequency (strong modulation limit<sup>9,27–29</sup>) within the stationary distribution, which means that the frequency fluctuation is noncorrelated. Of course the strength of the modulation can also be intermediate between these two limits.

The effects of frequency fluctuations in the weak modulation limit have been described analytically for a Gauss-Markov stochastic process<sup>8,15–26</sup> which is a frequency fluctuation process in which the stationary distribution is Gaussian and the correlation function for the detuning as given in Eq. (3.1) decays exponentially. This description has been applied to several optical techniques.<sup>16–26</sup> In a time-integrated FWM experiment, the frequency fluctuation in the weak modulation limit will lead to a transition from a nonexponential decay [with  $e^{-4D^2\tau^3/3T_c}$  (for  $\tau \ll T_c$ )] to an exponential decay [with  $e^{-2D^2T_c\tau}$  (for  $\tau \gg T_c$ )].<sup>17–20</sup> Hence the frequency fluctuation leads to a strong observable nonexponential decay of the third-order polarization if  $T_c$  is on the order of or larger than  $D^{-1}$ . Recently, two experimental FWM studies<sup>12,13</sup> confirmed the description of Refs. 17–20 for the effects of a frequency fluctuation in the weak modulation limit.

The effects of frequency fluctuations in the strong modulation limit have been described for free-induction decay<sup>9,27,29</sup> and FWM.<sup>28</sup> In a two-pulse self-diffracted FWM experiment, a frequency fluctuation in the strong modulation limit will only lead to a nonexponential decay for very small delays, irrespective of the value of  $T_c$ .<sup>28</sup> Hence, in this limit it is very difficult to determine whether the absorption line is homogeneously broadened, inhomogeneously broadened, or of intermediate character. However, in a three-pulse FWM experiment, the frequency fluctuation will lead to a strong nonexponential decay if  $T_c \gg D^{-1}$ . This non-exponential decay is due to the effects of the frequency fluctuation on the population grating that exists between the second and the third pulse. The effects of a fluctuation of the transition frequency on population gratings is often denoted as spectral diffusion.<sup>30–33</sup> The spectral diffusion models of Refs. 30–33 only consider the effects of the frequency fluctuation on the population grating. The rate of this modulation is defined with a time constant  $T_3$  that is exactly the same as the time constant  $T_c$ .

### B. Optical Bloch equations for three-pulse four-wave mixing

The system is described as a spectral distribution of two-level systems with transition frequency  $\omega$ . In this description we will not incorporate the effects of many-body Coulomb interactions between the excited excitons.<sup>34</sup> The optical Bloch equations for the polarization and the population of these two-level systems can be obtained directly from the time-dependent Schrödinger equation:

$$(H_{\text{sys}} + H_{\text{em}}) \Psi(t) = i\hbar \frac{\partial \Psi}{\partial t}, \quad (3.2)$$

with  $H_{\text{sys}}$  the Hamiltonian of the system,  $\Psi(t)$  the time-dependent wave function, and  $H_{\text{em}}$  the Hamiltonian of the electromagnetic field. In the electric dipole approximation, the Hamiltonian  $H_{\text{em}}$  equals  $e \sum_n r_n E \cos(\omega t)$  with  $e$  the elementary charge,  $r_n$  the position operator of the  $n$ th electron,  $E$  the envelope function of the electric field, and  $\omega$  the central frequency of the electromagnetic field.

The electromagnetic field can induce a transition between the two eigenstates of  $H_{\text{sys}}$  with time-independent wave functions  $\phi_1$  and  $\phi_2$  ( $H_{\text{sys}}\phi_1 = \hbar\omega_1\phi_1$  and  $H_{\text{sys}}\phi_2 = \hbar\omega_2\phi_2$ ). The time-dependent wave function  $\Psi(t)$  can then be written as

$$\Psi(t) = C_1(t)\psi_1(t) + C_2(t)\psi_2(t) \quad (3.3)$$

with  $\psi_j(t) = \phi_j e^{-i\omega_j t}$ . The optical Bloch equations are obtained by substituting Eq. (3.3) into Eq. (3.2). The optical Bloch matrix element  $\rho_{ij}(\omega)$  is defined as  $C_i C_j^*$ , with  $\omega$  equal to  $\omega_2 - \omega_1$ . When we substitute  $\tilde{\rho}_{21} e^{i(\omega - \omega_1)t}$  for  $\rho_{21}(\omega)$  and we neglect the rapidly oscillating terms (rotating-wave approximation), we obtain the following equations for the optical Bloch matrix elements:

$$\frac{\partial \tilde{\rho}_{21}(\omega)}{\partial t} = \frac{\partial \tilde{\rho}_{12}^*(\omega)}{\partial t} = -\frac{i}{2} V [\rho_{11}(\omega) - \rho_{22}(\omega)] - i(\omega - \omega_1) \tilde{\rho}_{21}(\omega), \quad (3.4a)$$

$$\frac{\partial \rho_{22}(\omega)}{\partial t} = -\frac{\partial \rho_{11}(\omega)}{\partial t} = \frac{i}{2} [V^* \tilde{\rho}_{21}(\omega) - V \tilde{\rho}_{12}(\omega)], \quad (3.4b)$$

with  $V = -\mu_{21} E / \hbar$ ,  $\mu_{21} = -e \langle \phi_2 | \sum_n r_n | \phi_1 \rangle$ .

The polarization  $\mathcal{P}$  is related to the off-diagonal optical Bloch matrix element  $\rho_{21}(\omega)$  through  $\mathcal{P} = N \{ \mu_{12} \int d\omega \rho_{21}(\omega) e^{-i\omega t} + \text{c.c.} \}$  with  $N$  the number density. The transition dipole moment  $\mu_{12}$  is assumed not to depend on the transition frequency  $\omega$ . When  $\mathcal{P}$  is written as  $\frac{1}{2} \{ P e^{-i\omega t} + \text{c.c.} \}$ , the envelope function  $P$  is equal to  $2N\mu_{12} \int d\omega \tilde{\rho}_{21}(\omega)$ . The population of the excited state is given by the diagonal optical Bloch matrix element  $\rho_{22}(\omega)$ .

The optical Bloch equations (3.4) do not contain any relaxation mechanisms. However, the stochastic modulation of the transition frequencies will lead to a decay and a gain of  $\tilde{\rho}_{21}(\omega)$  and  $\rho_{22}(\omega)$  at each particular  $\omega$ . The decay is assumed to be exponential with a time constant  $2T_c$  for  $\tilde{\rho}_{21}(\omega)$  and  $T_c$  for  $\rho_{22}(\omega)$ , where  $T_c$  is defined as in Eq. (1.1). The total decay of the polarization is given by  $\int d\omega' \tilde{\rho}_{21}(\omega') / 2T_c$ . This total amount of  $\tilde{\rho}_{21}$  is redistributed over all  $\tilde{\rho}_{21}(\omega)$  according to a spectral redistribution function  $F(\omega, \omega')$ . The function  $F(\omega, \omega')$  is normalized [ $\int d\omega' F(\omega, \omega') = 1$ ]. The gain of  $\tilde{\rho}_{21}(\omega)$  is thus given by  $\int d\omega' F(\omega, \omega') \tilde{\rho}_{21}(\omega') / 2T_c$ . The shape of  $F(\omega, \omega')$  determines whether the system is in the weak or in the strong modulation limit. If the value of  $F(\omega, \omega')$  rapidly drops when  $\omega'$  becomes different from  $\omega$ , the modulation is weak and many jumps of the frequencies are required before the frequency is significantly changed from its original value. If  $F(\omega, \omega')$  does not depend on  $\omega'$ , the modulation is very strong and the function  $F(\omega, \omega')$  be-

comes equal to the stationary distribution. In this limit the gain of  $\tilde{\rho}_{21}(\omega)$  due to spectral redistribution is given by  $F(\omega) \int d\omega' \tilde{\rho}_{21}(\omega')/2T_c$ . A similar description can be used to describe the effects of a stochastic modulation on the population.

The dynamics of the polarization and the population can be described with a number of frequency-fluctuation processes that all have their own characteristic values for  $T_c$  and the spectral width  $D$  and their characteristic form of  $F(\omega, \omega')$ . However, for frequency-fluctuation processes for which  $T_c$  is very small or very large compared to  $\tau_{\text{inh}}$  ( $= D^{-1}$ ), a simple homogeneous or inhomogeneous description suffices. We will assume that there is only one frequency-fluctuation process with an intermediate value for  $T_c$ . This  $T_c$  is allowed to be frequency dependent. In the following we will denote this frequency-fluctuation process with intermediate  $T_c$  as a spectral-migration process. For excitons in a quantum well, such a process can result from the migration of the excitons along the boundary between the quantum well and the barrier.

We assume that in addition to this spectral-migration process there is another process with a  $T_c$  that is very small compared to its characteristic  $\tau_{\text{inh}}$ . If  $T_c$  is very small compared to  $\tau_{\text{inh}}$ , the exchange of frequency components is so fast that the phases of  $\tilde{\rho}_{21}(\omega)$  no longer evolve with  $\omega$  and become locked. The sum of all  $\tilde{\rho}_{21}(\omega)$  will decay exponentially with a time constant  $T_2'$  that is equal to  $2D^2T_c^{-1}$  both in the weak and in the strong modulation limit. Such a very fast frequency-fluctuation process can result from the interactions of excitons with

acoustic phonons.

A third possible relaxation process that will influence the dynamics of the polarization and the population is formed by the decay of the excited-state population. Such a decay can be caused by radiative recombination of the exciton. Although this process will not lead to a fluctuation of the transition frequencies, it will still contribute both to the decay of the polarization and the population grating. The decay of the population due to population relaxation is accounted for with an exponential relaxation-time constant  $T_1$ . The decay of the polarization due to population relaxation is accounted for by incorporating  $T_1$  in the time constant of the homogeneous dephasing:  $1/T_2 = 1/T_2' + 1/2T_1$ .

We will describe the generation of the third-order polarization in the direction  $k_4 = k_3 + k_2 - k_1$  by a sequence of three laser pulses with a perturbation approach which implies that the  $n$ th-order optical Bloch matrix element is proportional to the  $n$ th power of the applied electromagnetic field.<sup>35</sup> The initial spectral distribution of two-level systems is given by the zeroth-order diagonal optical Bloch matrix elements  $\rho_{11}^{(0)}$  and  $\rho_{22}^{(0)}$ . The linear polarization  $\mathcal{P}^{(1)}$  is given by  $2N\tilde{\rho}_{21}^{(1)}(\omega)\mu_{12}$ . Similarly, the third-order polarization is given by  $2N\tilde{\rho}_{21}^{(3)}(\omega)\mu_{12}$ . The population grating is given by the second-order diagonal optical Bloch matrix element  $\rho_{22}^{(2)}(\omega)$ . Using the perturbation approach and introducing the three relaxation processes with time constants  $T_c$ ,  $T_2$ , and  $T_1$ , we obtain the following equations for a three-pulse FWM experiment:

$$\frac{\partial \tilde{\rho}_{21}^{(1)}(k_j, \omega)}{\partial t} = \frac{-i}{2} V_j(t) [\rho_{11}^{(0)}(\omega) - \rho_{22}^{(0)}(\omega)] - i(\omega - \omega_l) \tilde{\rho}_{21}^{(1)}(\omega) - \tilde{\rho}_{21}^{(1)}(\omega) \left( \frac{1}{T_2} + \frac{1}{2T_c(\omega)} \right) + \int d\omega' F(\omega, \omega') \frac{\tilde{\rho}_{21}^{(1)}(\omega')}{2T_c(\omega')}, \quad (3.5a)$$

$$\frac{\partial \rho_{22}^{(20)}(k_j - k_i, \omega)}{\partial t} = \frac{i}{2} \left[ V_i^*(t) \tilde{\rho}_{21}^{(1)}(k_j, \omega) - V_j(t) \tilde{\rho}_{12}^{(1)}(-k_i, \omega) \right] - \rho_{22}^{(2)}(\omega) \left( \frac{1}{T_1} + \frac{1}{T_c(\omega)} \right) + \int d\omega' F(\omega, \omega') \frac{\rho_{22}^{(2)}(\omega')}{T_c(\omega')}, \quad (3.5b)$$

$$\begin{aligned} \frac{\partial \tilde{\rho}_{21}^{(3)}(k_3 + k_2 - k_1, \omega)}{\partial t} &= i[V_3(t)\rho_{22}^{(2)}(k_2 - k_1, \omega)] + i[V_2(t)\rho_{22}^{(2)}(k_3 - k_1, \omega)] - i(\omega - \omega_l)\tilde{\rho}_{21}^{(3)}(\omega) \\ &\quad - \tilde{\rho}_{21}^{(3)}(\omega) \left( \frac{1}{T_2} + \frac{1}{2T_c(\omega)} \right) + \int d\omega' F(\omega, \omega') \frac{\tilde{\rho}_{21}^{(3)}(\omega')}{2T_c(\omega')}, \end{aligned} \quad (3.5c)$$

with the indices  $i$  and  $j$  denoting pulses 1, 2, and 3. The envelope function  $E_j$  is given by  $E_0 e^{-[(t-\tau_j)^2/\tau_p]^2}$  with  $\tau_j$  the delay of pulse  $j$  and  $\tau_p$  the pulse duration.

The coupled differential equations (3.5) are numerically solved using a fourth-order Runge-Kutta method implemented on a 486-33 personal computer. A typical simulation of a FWM experiment in which the time-integrated third-order polarization is calculated at 90 delays takes about 10 min.

Equations (3.5) form a general description for the generation and decay of the linear polarization, the popula-

tion grating, and the third-order polarization. The equations can be used irrespective whether the relaxation induced by the stochastic modulation is of homogeneous, inhomogeneous, or intermediate character. In addition, the stochastic modulation can be weak, strong, or of intermediate modulation strength. The main difference of Eqs. (3.5) with a spectral diffusion model<sup>30-33</sup> is formed by the terms  $\int d\omega' F(\omega, \omega') \tilde{\rho}_{21}(\omega')/2T_c(\omega')$  in the equations for the linear and the third-order off-diagonal optical Bloch matrix elements. In a spectral diffusion model these terms are absent, which means that these mod-

els assume that the linear and the nonlinear polarization only decay as a result of purely homogeneous and inhomogeneous dephasing processes.

#### IV. RESULTS AND DISCUSSION

##### A. Time-integrated three-pulse FWM experiments

In Fig. 2 the results of the time-integrated three-pulse FWM experiments are presented in a contour plot as a function of the delay  $T_{12}$  ( $= \tau_2 - \tau_1$ ) between pulse 1 and pulse 2 and the delay  $T_{23}$  ( $= \tau_3 - \tau_2$ ) between pulse 2 and pulse 3. Figure 3(a) presents four measurements in which  $T_{12}$  is varied and  $T_{23}$  is kept constant. Figure 3(b) presents four measurements in which  $T_{23}$  is varied and  $T_{12}$  is kept constant. In both Figs. 3(a) and 3(b) a strongly nonexponential decay is observed, indicative of a spectral-migration process with a time constant  $T_c$  on a picosecond time scale. If the absorption would have

been simply homogeneously and inhomogeneously broadened, the relaxation would have been purely exponential with a time constant  $T_2/4$  in the case of strong inhomogeneous broadening and  $T_2/2$  in the case of strong homogeneous broadening. If the spectral-migration process is in the weak modulation limit, an increase in the rate of decay is expected in the experiments in which  $T_{12}$  is varied.<sup>17–20</sup> If the spectral-migration process is in the strong modulation limit, a transition from a fast Gaussian to a slower exponential decay is expected in the experiments in which  $T_{12}$  is varied. The latter relaxation behavior is observed in Fig. 3(a) so that the modulation in the spectral-migration process must be strong, which implies that the jumps of the frequency in the frequency-fluctuation process are large and the width of the spectral redistribution function  $F$  is similar to the width of the initial spectral distribution  $\rho_{11}^{(0)}(\omega)$ . As a result, the function  $F(\omega, \omega')$  does not depend on  $\omega'$  and the spectral redistribution terms  $\int d\omega' F(\omega, \omega') \rho(\omega')$  in Eqs. (3.5a)–(3.5c) can be written as  $F(\omega) \int d\omega' \rho(\omega')$ .

The measurements are compared with calculations obtained with the model of the previous section. The dashed curves in Figs. 3(a) and 3(b) represent calculations of the signal using the model of Sec. III. All the simulations presented in Figs. 3(a) and 3(b) are carried out with the same values for  $T_c$  and  $T_2$ . In all the calculations we assumed an equal (Gaussian) spectral de-

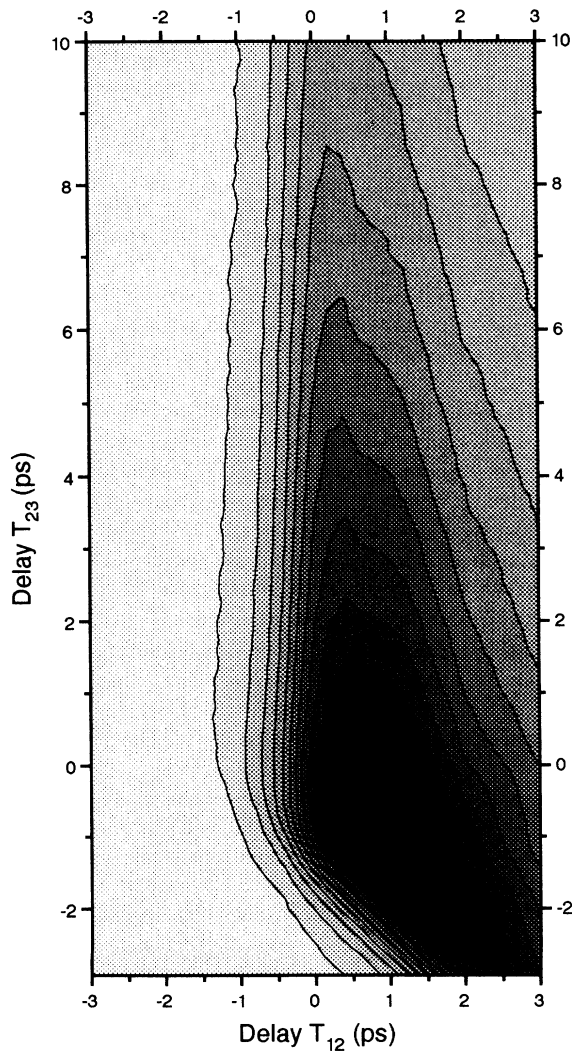


FIG. 2. Time-integrated three-pulse four-wave-mixing signal as a function of the delay  $T_{12}$  between pulse 1 and pulse 2 and delay  $T_{23}$  between pulse 2 and pulse 3.

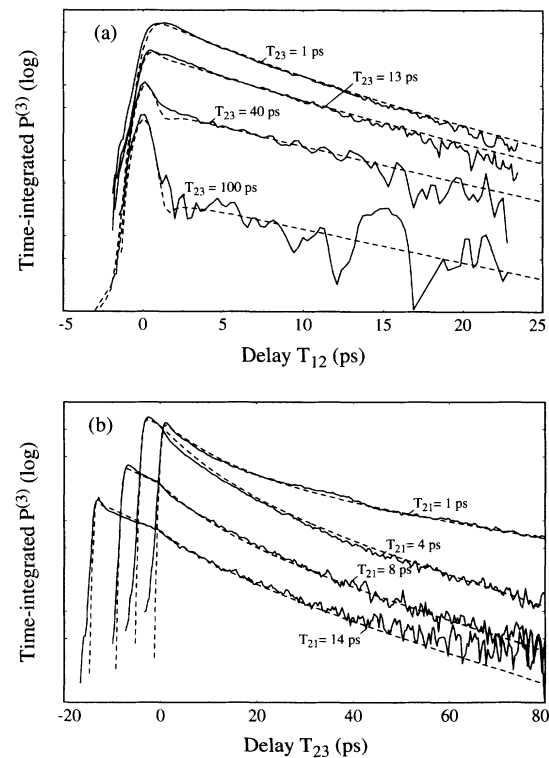


FIG. 3. Time-integrated three-pulse four-wave-mixing signal. The dashed curves represent numerical simulations of the measurements using the model of Sec. III. In (a) the delay  $T_{12}$  between pulse 1 and pulse 2 is varied while the delay  $T_{23}$  between pulse 2 and 3 is kept constant. In (b) the delay  $T_{23}$  is varied while the delay  $T_{12}$  is kept constant.

pendence for  $\rho_{11}^{(0)}(\omega)$ ,  $\rho_{22}^{(0)}(\omega)$ , and  $F(\omega)$ , all centered at  $\omega_0$  and with a width of 0.75 THz (3.1 meV). The calculations are performed assuming 500-fs Gaussian shaped pulses. We found that the experiments could be fitted well without incorporating the effects of population relaxation ( $T_1 = \infty$ ). We took  $T_c$  to be frequency dependent, varying between 56 ps for low-energy excitons to 9 ps for high-energy excitons. The value of the time constant  $T_c$  of the spectral-migration process is much larger than  $\tau_{\text{inh}}$  ( $= 350$  fs for a spectral width of 0.75 THz), which implies that the frequency fluctuation is close to the inhomogeneous limit. Nevertheless, the observed relaxation behavior strongly differs from the simple exponential decay that would result if the time constant  $T_c$  would have been infinitely large. As a result of the strong inhomogeneous character, the signal in the diffracted direction is mainly formed by a photon echo and the signal in Fig. 3(a) is strongly asymmetric as a function of  $T_{12}$ . For  $T_2$  we used a value of 70 ps.

### 1. Variation of the delay between pulse 1 and 2

In Fig. 3(a) we observe that for large constant  $T_{23}$  the signal shows a rapid Gaussian decay as a function of  $T_{12}$ . This observation can be understood as follows. The spectral redistribution between the second and the third pulse will lead to a decay of each  $\rho_{22}^{(2)}(\omega)$  until  $\rho_{22}^{(2)}(\omega)/T_c(\omega)$  becomes equal to  $F(\omega) \int d\omega' \rho_{22}^{(2)}(\omega')/T_c(\omega')$ . If  $T_c$  would not depend on frequency, each  $\rho_{22}^{(2)}(\omega)$  would finally decay to a value  $F(\omega) \int d\omega' \rho_{22}^{(2)}(\omega')$ . The value of the latter integral has a Gaussian dependence on  $T_{12}$  and becomes equal to zero for  $T_{12} \gg \tau_{\text{inh}}$ . As a result, all  $\rho_{22}^{(2)}(\omega)$  will decay to  $e^{-T_{23}/T_c}$  their initial value if  $T_{12} \gg \tau_{\text{inh}}$  and will not decay at all if  $T_{12} \ll \tau_{\text{inh}}$ . Hence, if  $T_{23}$  is large, the population grating and the generated polarization will show a clear initial Gaussian decay as a function of  $T_{12}$ .

In addition to the decay of the population grating, the diffracted intensity decreases due to the decay of the  $\tilde{\rho}_{12}^{(1)}(-k_1, \omega)$  between pulse 1 and pulse 2 and the decay of  $\tilde{\rho}_{21}^{(3)}(k_3 + k_2 - k_1, \omega)$  before the photon echo is formed. For  $T_{12} \gg \tau_{\text{inh}}$  the values of  $\int d\omega' \tilde{\rho}_{12}^{(1)}(-k_1, \omega')/2T_c(\omega')$  and  $\int d\omega' \rho_{22}^{(2)}(k_2 - k_1, \omega')/T_c(\omega')$  become very small. In that limit the intensity of the photon echo decays exponentially with a time constant  $1/(4/T_2 + 2/T_c)$ , if  $T_c$  would be frequency independent. However, we observe in Fig. 3(a) that the time constant of the exponential decay increases with increasing  $T_{23}$ . In addition, we observe that for  $T_{23} = 1$  ps the decay of the signal is nonexponential, even when  $T_{12}$  is larger than  $\tau_{\text{inh}}$ . These observations indicate that the different frequencies in the spectral distribution have different values of  $T_c$ . If the spectral distribution contains frequency components with different values for  $T_c$ , the dynamics of the signal will be dominated by the frequency components with a small  $T_c$  for small  $T_{12}$  and small  $T_{23}$  and by the frequency components with a large  $T_c$  for large  $T_{12}$  or large  $T_{23}$ . Hence, for small  $T_{23}$ , the observed time constant of the relaxation will increase with increasing  $T_{12}$  as is indeed observed in

Fig. 3(a). If  $T_{23}$  is large, the third-order polarization generated by the third pulse will be strongly dominated by  $\rho_{22}^{(2)}(k_2 - k_1, \omega)$  at frequencies  $\omega$  for which  $T_c$  is large. Therefore the time constant of the decay for  $T_{12} \gg \tau_{\text{inh}}$  will become larger with increasing  $T_{23}$ , which is also observed in Fig. 3(a). We find that the experimental results in Figs. 3(a) and 3(b) can be fitted well with a  $T_c$  of 56 ps for low-energy excitons and 9 ps for high-energy excitons. The frequency dependence of  $T_c$  is presented in Fig. 4. We assume that the transition from 56 to 9 ps has a linear dependence on frequency. We find that the exact shape of this transition is not very critical. In contrast, the value of the central frequency of this transition strongly influences the shape of the measured signal because this frequency determines the relative amount of rapidly and slowly spectrally migrating excitons. The time constant of 56 ps for low-energy excitons agrees very well with the value of 60 ps that has been found previously for the spectral redistribution of localized excitons in a GaAs/AlGaAs multiple-quantum-well structure.<sup>33</sup> This time constant is also in good agreement with the time constant that is calculated for the phonon-assisted migration of localized excitons.<sup>36</sup> The time constant of 9 ps for high-energy excitons can be explained from the phonon-assisted migration of delocalized excitons.

### 2. Variation of the delay between pulse 2 and 3

In the experiments of Fig. 3(b) two regimes can be distinguished. In the first regime pulse 3 enters the sample between pulse 1 and pulse 2 ( $T_{23} < 0$ ). In this regime the population grating is formed by pulses 1 and 3 and pulse 2 is diffracted from this grating. In the second regime pulse 3 enters after pulse 2 ( $T_{23} > 0$ ) and pulses 1 and 2 will form the grating from which pulse 3 is diffracted. If the absorption would have been homogeneously and inhomogeneously broadened, the decay would have been purely exponential in the first regime and no decay would have been observed in the second regime (when  $T_1 = \infty$ ). However, we observe a strongly nonexponential decay in the second regime, which shows the presence of a spectral-migration process with a time constant on a picosecond time scale. If pulse 3 enters shortly after pulse 1, the  $\tilde{\rho}_{12}^{(1)}(-k_1, \omega)$  generated by pulse 1 will not be dephased before the population grating is formed, so that the spectral redistribution between pulse 3 and pulse 2 hardly leads to a decay of the signal. This explains the small peak in the signal measured with  $T_{12} = 14$  ps at a delay  $T_{23}$  of  $-14$  ps. We also observe in all measurements of Fig. 3(b) that the signal shows a relatively slow decay as a function of  $T_{23}$  when pulse 3 enters the sample between pulse 1 and 2. This can be understood in the following way. The diffracted signal will decay as a function of  $T_{23}$  due to the decay of  $\tilde{\rho}_{12}^{(1)}(-k_1, \omega)$  between pulse 1 and 3 and the decay of  $\tilde{\rho}_{21}^{(3)}(k_3 + k_2 - k_1, \omega)$  before the photon echo is formed. For  $T_{13} \gg \tau_{\text{inh}}$ , this decay will be exponential with time constant  $1/(4/T_2 + 2/T_c)$ . However, if pulse 3 enters the sample between pulse 1 and 2, the signal will rise with increasing  $T_{23}$  due to the smaller decay of the population grating between pulse 3

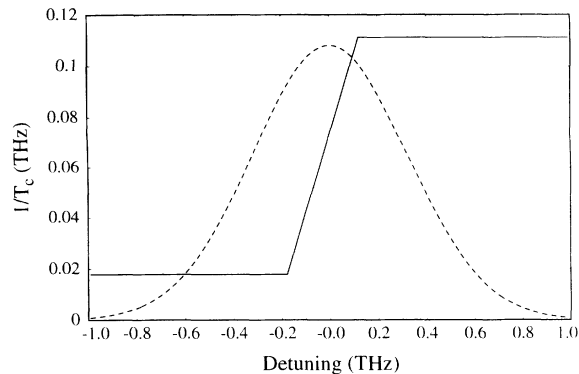


FIG. 4. Spectral dependence of the time constant  $T_c$  for the modulation of the transition frequency. The dashed curve represents the spectral distribution used in the calculation of the third-order nonlinear response of the heavy-hole exciton.

and pulse 2. For  $T_{13} \gg \tau_{\text{inh}}$ , this rise of the diffracted signal will be exponential with time constant  $T_c/2$ . The rate of decay observed in the experiment will be the difference between the two processes and will thus be exponential with a time constant  $T_2/4$ . Hence the value of the time constant  $T_2$  of the homogeneous dephasing can be accurately determined from the measurement of the decay of the diffracted signal as a function of  $T_{23}$  for constant  $T_{12}$ .

From the simulation of the measurements in Fig. 3(b) we deduce that  $T_2$  is 70 ps. This value was also used in the simulation of the measurements of Fig. 3(a). The value of 70 ps is large compared to the time constant  $T_c$  of the spectral migration of high-energy excitons. This means that the decay of the polarization as a function of  $T_{12}$  as measured in Fig. 3(a) is *strongly dominated by the spectral migration of the delocalized excitons*.

We were able to determine the contribution of the homogeneous processes to the dephasing due to the fact that a spectral-migration process leads to a decay of both the polarization and the population grating whereas a homogeneous dephasing process only induces a decay of the polarization and does not affect the population grating. This can be understood in the following way. Both the spectral migration and the homogeneous dephasing process can be modeled as frequency fluctuation processes with characteristic values for  $T_c$  and the width of the spectral distribution. The simultaneous occurrence of both processes can be modeled by describing each frequency component in the spectral distribution of the spectral-migration process as a spectral distribution of the homogeneous dephasing process. For a purely homogeneous dephasing process the fluctuations are infinitely fast so that the phases of  $\tilde{\rho}_{12}^{(1)}(\omega)$  within the spectral distribution of the homogeneous process will remain the same. As a result, the  $\rho_{22}^{(2)}(\omega)$  generated by the second pulse will also all have the same phase. The spectral redistribution between pulse 2 and 3 leads to a decay of each  $\rho_{22}^{(2)}(\omega)$  to a limiting value of  $F(\omega) \int \rho_{22}^{(2)}(\omega) d\omega$  (in the strong modulation limit). If all  $\rho_{22}^{(2)}(\omega)$  have the same phase, the value of  $\rho_{22}^{(2)}(\omega)$  is exactly equal to  $F(\omega) \int \rho_{22}^{(2)}(\omega) d\omega$ . Therefore, the very rapid fluctuations within the spectral distribution of the homogeneous pro-

cess will only lead to a decay of the polarization and do not affect the population grating. For the spectral-migration process, the value of  $T_c$  is large compared to  $D^{-1}$  so that the  $\tilde{\rho}_{12}^{(1)}(\omega)$  will rapidly dephase. The value of  $\int \rho_{22}^{(2)}(\omega) d\omega$  will be small if the delay between the first two pulses is larger than  $D^{-1}$  so that the spectral redistribution between the second and the third pulse will lead to a decay of all  $\rho_{22}^{(2)}(\omega)$ . As a result, a spectral-migration process induces a decay of both the polarization and the population grating. Therefore, with a time-integrated three-pulse FWM experiment, in which the signal is determined by the dynamics of both the polarization and the population grating, it is possible to distinguish between the contributions of homogeneous dephasing and spectral-migration processes to the observed dephasing.

If pulse 3 enters after pulse 2 ( $T_{23} > 0$ ), we observe a nonexponential decay of the signal as a function of  $T_{23}$ . For small  $T_{12}$  the decay can be nonexponential because in that case the spectral redistribution between pulse 2 and 3 leads to a decay of each  $\rho_{22}^{(2)}(k_2 - k_1, \omega)$  to a final value of  $F(\omega) \int d\omega' \rho_{22}^{(2)}(k_2 - k_1, \omega')$ . This is observed in Fig. 3(b) for  $T_{12} = 1$  ps. If  $T_{12} = 0$  ps, one would expect that the signal does not decay at all as a function of  $T_{23}$  because all  $\rho_{22}^{(2)}(k_2 - k_1, \omega)$  remain in phase. However, due to the limited bandwidth of the pulses, the central frequency components of the absorption band are more efficiently excited than the frequency components in the wings of the absorption band. The spectral redistribution between pulse 2 and pulse 3 makes that the initially excited narrow frequency distribution of the population grating will gradually change into the broader distribution as defined by  $F(\omega)$ . Due to the limited bandwidth of the third pulse, this broader distribution is less efficiently transferred into a third-order polarization although  $\int d\omega' \rho_{22}^{(2)}(k_2 - k_1, \omega')/T_c$  is still the same.

For  $T_{12} \gg \tau_{\text{inh}}$  the value of  $\int d\omega' \rho_{22}^{(2)}(k_2 - k_1, \omega')/T_c$  becomes very small so that the diffracted intensity should decay exponentially as a function of  $T_{23}$  with a time constant  $T_c/2$ . However, we observe in Fig. 3(b) that even for large  $T_{12}$  the decay appears to be nonexponential. This nonexponential decay for  $T_{12} \gg \tau_{\text{inh}}$  shows that for small  $T_{23}$  the decay is strongly influenced by frequency components that have a small  $T_c$  whereas for large  $T_{23}$  the decay is dominated by frequency components with large  $T_c$ .

## B. Time dependence of the spectral distribution

The different time constants  $T_c$  for the low-energy and the high-energy side of the absorption band not only lead to a transition from a fast to a slow exponential decay but also to a shift of the excited spectral distribution to lower energies with increasing delay. In Fig. 5(a) the spectral distribution of  $|\tilde{\rho}_{21}^{(3)}(\omega)|^2$  at the time of the photon echo ( $t = \tau_3 + \tau_2 - \tau_1$ ) is presented for three different values of  $T_{12}$  and  $T_{23} = 0$  ps. In Fig. 5(b) this spectral distribution is presented for three different values of  $T_{23}$  and  $T_{12} = 0$  ps. In both figures a shift of the excited

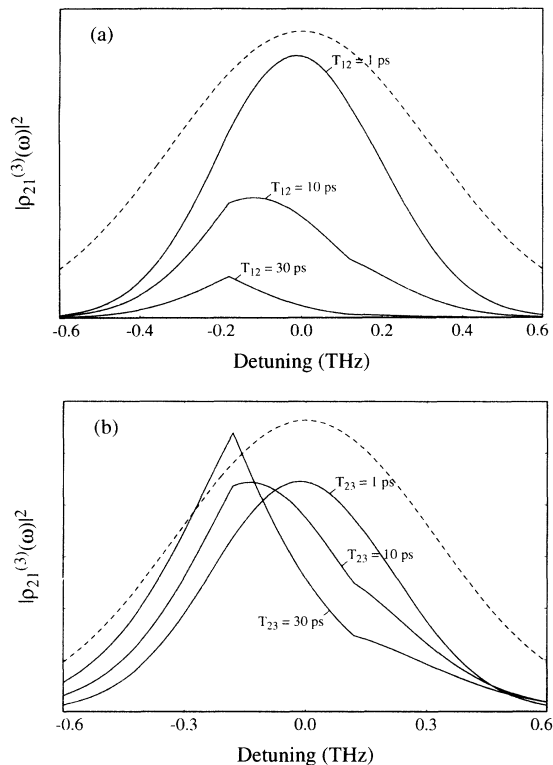


FIG. 5. Spectral distribution of  $|\rho_{21}^{(3)}(\omega)|^2$  at the maximum of the photon echo ( $t = \tau_3 + \tau_2 - \tau_1$ ). In (a) the spectral distributions are shown at three different values of  $T_{12}$  with  $T_{23} = 0$  ps and in (b) at three different values of  $T_{23}$  with  $T_{12} = 0$  ps. The dashed curve represents the spectral distribution used in the calculation.

spectral distribution to lower energies is observed with increasing delay. It is also observed in both figures that the excited spectral distribution is narrower than the absorption line due to the fact that the used laser pulses are not infinitely short. The kinks in these figures are due to the fact that we assumed in the calculation that the time constant  $T_c$  changes linearly from 56 ps to 9 ps. In Fig. 5(a) the signal strongly decreases with increasing  $T_{12}$  due to the fluctuation of the transition frequency with time constant  $T_c$  and the homogeneous dephasing with time constant  $T_2$ . In contrast, in Fig. 5(b) the signal hardly decays with increasing  $T_{23}$ . In this figure the value of  $T_{12}$  was taken equal to 0 ps so that the  $\tilde{\rho}_{12}^{(1)}(-k_1, \omega)$  are still in phase as they are transferred into a population grating by pulse 2. Hence the value of  $\int d\omega' \rho_{22}^{(2)}(\omega')/T_c(\omega')$  will be large and the spectral redistribution will hardly lead to a decay of the population grating. Due to the frequency dependence of  $T_c$  the loss will be larger than the gain at high frequencies whereas the gain will be larger than the loss at low frequencies so that the spectral distribution will shift to lower energies with increasing  $T_{23}$ .

### C. Discussion

We find that the observed nonexponential decay of the excitons results from a spectral-migration process in

the strong modulation limit. In previous studies on dye molecules in solution<sup>12,13</sup> it was found that the nonexponential decay resulted from a spectral-migration process in the weak modulation limit. The stochastic modulation for dye molecules in solution will be weak because in the liquid phase the frequency fluctuation is due to small reorientations of the molecules. The fact that we observe a strong frequency fluctuation for the excitons in quantum wells shows that the boundaries of the quantum wells and the barriers possess a certain roughness, which allows the excitons to change their frequency by a rather large amount within a small distance along the interface. The migration along the interface is probably phonon induced.<sup>36</sup> However, the data obtained in the present experiment do not allow an unambiguous identification of the microscopic processes that induce the strong fluctuation of the transition frequency.

The relaxation behavior of the third-order polarization for a single spectral-migration process for which  $T_c \approx \tau_{inh}$  strongly differs from the relaxation behavior for an absorption line that is both homogeneously and inhomogeneously broadened. The third-order polarization is formed by either a photon echo, a free-induction decay or a signal in between, but never by both a photon echo and a free-induction decay. This is also the case if the broadening of the absorption line results from a single spectral-migration process with  $T_c \approx \tau_{inh}$  in the weak modulation limit. However, in the strong modulation limit, we calculate that the third-order polarization can be formed by a simultaneous photon echo and free-induction decay. The simultaneous occurrence of a free-induction decay and a photon echo has been observed experimentally and was explained by two spectrally overlapping homogeneously and inhomogeneously broadened absorption lines.<sup>37</sup> We believe that it is much more likely that this observation is caused by a single spectral-migration process in the strong modulation limit.

### V. CONCLUSIONS

We have investigated the dephasing mechanisms of excitons in GaAs/AlGaAs quantum wells with time-integrated three-pulse four-wave mixing. The experimental results are compared with a model for three-pulse FWM which provides a unified description of homogeneous dephasing, inhomogeneous dephasing, and spectral migration. We find that time-integrated three-pulse FWM can distinguish between the contributions to the dephasing of homogeneous dephasing and spectral migration. In addition, the strength of the modulation in the latter process can be determined.

We observe a nonexponential decay of the FWM signal that can be simulated well assuming a spectral-migration process in the strong modulation limit with a  $T_c$  of 56 ps for low-energy excitons and a  $T_c$  of 9 ps for high-energy excitons. The time constant of 56 ps agrees very well with the rate of phonon-induced migration that has been found previously for localized excitons. We find a frequency-independent value of 70 ps for the time constant  $T_2$  of the homogeneous dephasing. This value is large compared to the time constant of the spectral-



migration process. Therefore we conclude that the observed dephasing of excitons in quantum wells is dominated by a spectral-migration process that is much faster for delocalized excitons than for localized excitons. The observation that the spectral migration is in the strong modulation limit indicates that the frequency fluctuations may be the result of a phonon-induced migration of the excitons along the boundary of the quantum well and the barrier.

## ACKNOWLEDGMENTS

We thank the late S. Schmitt-Rink for stimulating the experimental investigations and, together with S. Mukamel, for many useful discussions about the theoretical aspects of four-wave mixing. Part of this work was supported by the Deutsche Forschungsgemeinschaft (Contract No. Le 747).

- <sup>1</sup> J. Shah, *IEEE J. Quantum Electron.* **24**, 276 (1988).
- <sup>2</sup> E. O. Göbel, *Festkörperprobleme (Advances in Solid State Physics)*, edited by U. Rossler (Vieweg, Braunschweig, 1990), Vol. 30, p. 269.
- <sup>3</sup> L. Schultheis, M. D. Sturge, and J. Hegarty, *Appl. Phys. Lett.* **47**, 995 (1985).
- <sup>4</sup> L. Schultheis, J. Kuhl, A. Honold, and C. W. Tu, *Phys. Rev. Lett.* **57**, 1635 (1986).
- <sup>5</sup> L. Schultheis, A. Honold, J. Kuhl, K. Köhler, and C. W. Tu, *Phys. Rev. B* **34**, 9027 (1986).
- <sup>6</sup> P. C. Becker, H. L. Fragnito, C. H. Brito-Cruz, R. L. Fork, J. E. Cunningham, J. E. Henry, and C. V. Shank, *Phys. Rev. Lett.* **61**, 1647 (1988).
- <sup>7</sup> N. Bloembergen, E. M. Purcell, and R. V. Pound, *Phys. Rev.* **73**, 679 (1948).
- <sup>8</sup> P. W. Anderson and P. R. Weiss, *Rev. Mod. Phys.* **25**, 269 (1953), P. W. Anderson, *J. Phys. Soc. Jpn.* **9**, 316 (1954).
- <sup>9</sup> R. Kubo, *J. Phys. Soc. Jpn.* **9**, 935 (1954).
- <sup>10</sup> J. T. Remillard, H. Wang, D. G. Steel, J. Oh, J. Pamulapati, and P. K. Bhattacharya, *Phys. Rev. Lett.* **62**, 2861 (1989).
- <sup>11</sup> H. Wang, M. Jiang, and D. G. Steel, *Phys. Rev. Lett.* **65**, 1255 (1990).
- <sup>12</sup> J.-Y. Bigot, M. T. Portella, R. W. Schoenlein, C. J. Bardeen, A. Migus, and C. V. Shank, *Phys. Rev. Lett.* **66**, 1138 (1991).
- <sup>13</sup> E. T. J. Nibbering, D. A. Wiersma, and K. Duppen, *Phys. Rev. Lett.* **66**, 2464 (1991).
- <sup>14</sup> K. Leo, J. Shah, E. O. Göbel, T. C. Damen, S. Schmitt-Rink, W. Schäfer, J. F. Müller, K. Köhler, and N. Garer, *Phys. Rev. B* **44**, 5726 (1991).
- <sup>15</sup> J. R. Klauder and P. W. Anderson, *Phys. Rev.* **125**, 912 (1962).
- <sup>16</sup> S. Mukamel, *Chem. Phys.* **37**, 33 (1979).
- <sup>17</sup> S. Mukamel, *Phys. Rev. A* **28**, 3480 (1983).
- <sup>18</sup> R. F. Loring and S. Mukamel, *Chem. Phys. Lett.* **114**, 426 (1985).
- <sup>19</sup> W. B. Bosma, Y. J. Yan, and S. Mukamel, *Phys. Rev. A* **42**, 6920 (1990).
- <sup>20</sup> Y. J. Yan and S. Mukamel, *J. Chem. Phys.* **94**, 179 (1991).
- <sup>21</sup> S. Mukamel, *J. Chem. Phys.* **82**, 5398 (1985); Y. J. Yan and S. Mukamel, *ibid.* **86**, 6085 (1987).
- <sup>22</sup> W. Vogel, D.-G. Welsch, and B. Wilhelmi, *Phys. Rev. A* **37**, 3825 (1988).
- <sup>23</sup> A. G. Kofman, R. Zaibel, A. M. Levine, and Y. Prior, *Phys. Rev. A* **41**, 6454 (1990).
- <sup>24</sup> W. B. Bosma, Y. J. Yan, and S. Mukamel, *J. Chem. Phys.* **93**, 3863 (1990).
- <sup>25</sup> E. T. J. Nibbering, K. Duppen, and D. A. Wiersma, *J. Chem. Phys.* **93**, 5477 (1990).
- <sup>26</sup> S. Schmitt-Rink, S. Mukamel, K. Leo, J. Shah, and D. S. Chemla, *Phys. Rev. A* **44**, 2124 (1991).
- <sup>27</sup> A. I. Burshtein, *Zh. Eksp. Teor. Fiz.* **62**, 1695 (1972) [*Sov. Phys. JETP* **35**, 882 (1972)].
- <sup>28</sup> A. B. Doktorov and A. I. Burshtein, *Zh. Eksp. Teor. Fiz.* **63**, 784 (1972) [*Sov. Phys. JETP* **36**, 411 (1973)].
- <sup>29</sup> A. I. Burshtein and V. S. Malinovsky, *J. Opt. Soc. Am. B* **8**, 1098 (1991).
- <sup>30</sup> A. M. Weiner, S. De Silvestri, and E. P. Ippen, *J. Opt. Soc. Am. B* **2**, 654 (1985).
- <sup>31</sup> T. Yajima and H. Souma, *Phys. Rev. A* **17**, 309 (1978).
- <sup>32</sup> H. Souma, E. Heilweil, and R. M. Hochstrasser, *J. Chem. Phys.* **76**, 5693 (1982).
- <sup>33</sup> H. Wang and D. G. Steel, *Phys. Rev. A* **43**, 3823 (1991).
- <sup>34</sup> M. Wegener, D. S. Chemla, S. Schmitt-Rink, and W. Schaefer, *Phys. Rev. A* **42**, 5675 (1990); C. Stafford, S. Schmitt-Rink, and W. Schaefer, *Phys. Rev. B* **41**, 10 000 (1990).
- <sup>35</sup> T. Yajima and Y. Tara, *J. Phys. Soc. Jpn.* **47**, 1620 (1979).
- <sup>36</sup> T. Takagahara, *J. Lumin.* **44**, 347 (1989).
- <sup>37</sup> M. D. Webb, S. T. Cundiff, and D. G. Steel, *Phys. Rev. Lett.* **66**, 934 (1991).

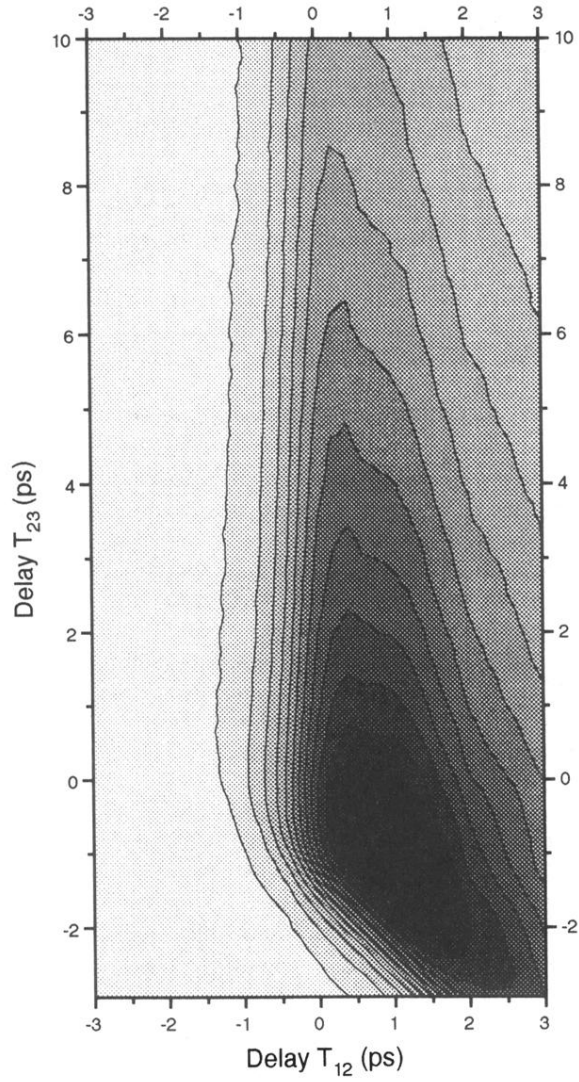


FIG. 2. Time-integrated three-pulse four-wave-mixing signal as a function of the delay  $T_{12}$  between pulse 1 and pulse 2 and delay  $T_{23}$  between pulse 2 and pulse 3.